Towards mid-infrared, sub-diffraction, spectral-mapping of human cells and tissue: SNIM (scanning near-field infrared microscopy) tip fabrication.

Giorgos S. Athanasiou, Johanna Ernst, David Furniss, Trevor M. Benson, Jasbinder Chauhan, John Middleton, Chris Parmenter, Mike Fay, Nigel Neate, Vladimir Shiryaev, Mikhail F. Churbanov and Angela B. Seddon*

***Abstract*— Scanning near-field infrared microscopy (SNIM) potentially enables sub-diffraction, broadband mid-infrared (MIR: 3-25 μm wavelength range) spectral-mapping of human cells and tissue for real-time molecular sensing, with prospective use in disease diagnosis. SNIM requires a MIR-transmitting tip of small aperture for photon collection. Here, chalcogenide-glass optical-fibers are reproducibly tapered at one end to form a MIR-transmitting tip for SNIM. A wet-etching method is used to form the tip. The tapering sides of the tip are Al-coated. These Al-coated tapered-tips exhibit near-field power-confinement when acting either as the launch-end or exit-end of the MIR optical fiber. We report first time optimal cleaving of the end of the tapered tip using Focused Ion Beam milling. A flat aperture is produced at the end of the tip, which is orthogonal to the fiber-axis and of controlled diameter. A FIB-cleaved aperture is used to collect MIR spectra of cells mounted on a transflection plate, under illumination of a synchrotron-generated wideband MIR beam.**

Keywords—chalcogenide glass, mid-infrared, chemical etching, fiber processing, transflection spectra)

I. INTRODUCTION

A. Scanning Near-Field Infrared Microscopy (SNIM)

According to Abbe [1], the diffraction limit of optical resolution of a focusing lens is directly proportional to the wavelength of light used, and inversely proportional to the lens numerical aperture.

Giorgos S. Athanasiou, Johanna Ernst, David Furniss, Trevor M. Benson and Angela B. Seddon* are with the Mid-Infrared Photonics Group, George Green Institute for Electromagnetics Research, Faculty of Engineering, University of Nottingham, University Park, Nottingham NG7 2RD, UK (* mail: angela.seddon@nottingham.ac.uk).

Jasbinder Chauhan[2] and John Middleton[2] are with the School of Physics and Astronomy, Faculty of Science, University of Nottingham, (address as above).

Chris Parmenter and Mike Fay are with the Nottingham Nanotechnology and Nanoscience Centre, Faculties of Science and Engineering, University of Nottingham, (address as above).

Nigel Neate is with the Department of Mechanical, Materials and Manufacturing, Faculty of Engineering, University of Nottingham, (address as above).

Vladimir Shiryaev and Mikhail F. Churbanov are with the Institute of Chemistry of High-Purity Substances of the Russian Academy of Sciences, Nizhny Novgorod, Russian Federation.

The optical resolution of visible-light microscopy is diffraction-limited to hundreds of nm. Microscopy at the longer wavelength range of ~3-12 μm considered here, part of the mid-infrared (MIR) (3-25 μm) spectral region, is diffraction limited to several μm. Advanced microscopy techniques, such as atomic force microscopy (AFM) and electron microscopy, go beyond the optical diffraction-limits but, on their own, fail to gather optical information from the sample.

Scanning near-field optical microscopy (SNOM) makes use of the van der Waals' attractive forces, in conjunction with a non-propagating optical evanescent field, at the sample-surface. SNOM overcomes the visible diffraction limit to obtain topological mapping of samples to a spatial resolution of10s nm [2]. The van der Waals' field intensity drops exponentially with increasing distance from the atomic surface of the sample. An atomically sharp tip rastered across a sample surface, using a piezoelectric stage, can maintain a constant tip distance from an atomically undulating sample surface, by means of either a normal force feedback mechanism, as in AFM, or a shear-force feedback - in which the tip is oscillated at its resonant frequency [2]. Collection of the evanescent optical field at the sample surface is by a photon-collector, held within nm of the sample surface, such as a tapered silica-glass optical fiber tip.

Scanning near-field infrared microscopy (SNIM) is an extrapolation of the SNOM technique into the MIR spectral region. This is attractive because MIR light stimulates the fundamental vibrational absorption of molecular species, which can be uniquely attributable, and has large extinction coefficients. SNIM enables molecular spectral-mapping of the sample surface beyond the diffraction limit giving direct spatial correlation between topographical and molecular information.

Broadband, black-body MIR sources, such as the Globar© (*based on an electrically heated ceramic bar*) are routinely used for FT-(*Fourier transform*)-IR spectroscopy, but provide insufficient brightness (*defined as power per unit area per unit solid angl*e) for SNIM. SNIM has been successfully demonstrated with a Free Electron Laser (FEL) [3-7] with a tunable output (2.1-9.8 μm wavelength). A tapered MIR-transmitting glass optical fiber tip was the photon-collector.

Topological and MIR spectral mapping to 50 and 100 nm resolution, respectively, were obtained.

Synchrotron-generated MIR broadband light is a 'pencil-beam' of a few mm diameter, can be focused to *ca.* 10 μm aperture, and is several orders of magnitude brighter than a Globar source at these small apertures. However, the synchrotron is non-portable. Recently we [8] and others [9] have reported new, MIR fiber-optic supercontinuum (SC) sources which can be very bright, of small aperture, and portable. Working towards a portable fiber-optic SNIM is an important reason for choosing SNIM tips that are part of a MIR fiber-optic system, as opposed to using stand-alone tips [10].

Human cells and tissue exhibit MIR spectral signatures due to their constituent biomolecules [11]. Our interest is to develop SNIM of human cells and tissue, with prospective use in disease diagnosis [12]. Thus it would be potentially possible to study exfoliated cells where disease is present and potentially to monitor the response of diseased cells to drug treatment.

B. MIR-transmitting Glass Tapered-tips for SNIM

Chalcogenide glasses are based on the chalcogen elements (Group XVI). They have low phonon energy, transparency within the wavelength range 0.6-25 μm [13, 14] and are robust enough for development as MIR fiber-optics' and SNIM tips. For instance, we have recently reported ultra-low (83 dB/km [15]) loss GeAsSe based optical fibers, exhibiting loss of<10 dB/m across 1-12 μm, which encompasses the region of interest for SNIM of human cells and tissue [11, 12].

Two techniques for making chalcogenide optical fiber tapered-tips have been reported [3, 5-7, 16]; (i)tapering fiber by 'thermal-stretching', applying axial stress to a fiber held > T_g (glass transition) [3, 6, 16] and (ii) wet-etching to taper the fiber end [3, 5, 7]. 'Thermal-stretching' with a micro-pipette-puller (P-2000, Sutter) [6] produced long tapered tips with large tip aperture; the high melt-fragility of the chalcogenide glass supercooled-melts implies temperature control is critical during stretching [16].

In the current work, Piranha wet-etching and propylamine wet-etching were compared. Piranha-etched, optical fiber, tapered-tips were aluminum-coated, to encourage MIR optical confinement during SNIM. The Al-coated, optical-fiber tapered-tips exhibited near-field power-confinement when acting either as the launch-end or exit-end of the MIR fiber. For the first time Focused Ion Beam (FIB) etching has been used to achieve optimal cleaving at the end of the tapered-fiber to form a controlled aperture which was flat, smooth, and orthogonal to the fiber-axis.

II. FABRICATION OF CHALCOGENIDE GLASS FIBER TAPERED-TIPS

Piranha wet-etching and propylamine wet-etching of unstructured TeAsSe chalcogenide-glass fiber were compared. The TeAsSe fiber was manufactured *via* preform-drawing at The University of Nottingham, UK.

Piranha etching was investigated of ultra-low loss step-index-fiber (SIF) of core/cladding AsSe/AsSeS fiber (hereafter called: AsSe-SIF) which was manufactured using melt-drawing at the Institute of Chemistry of High Purity Substances of the Russian Academy of Sciences, Russian Federation.

1. TeAsSe SNIM tips

A. TeAsSe fiber manufacture

$Te_{20}As_{30}Se_{50}$ (atomic% (at%)) glass was batched from ≥5×9s purity precursor elements: Te and Se (Cerac) and As (Furukawa Electric Ltd.) inside a MBraun glovebox (O_2 and H_2O each < 0.1 ppm), into a silica glass ampoule (GlobalQuartz),then sealed under vacuum (< 10^{-4}Pa). The ampoule had been prior-purified, by sequential heating in air, then under vacuum (< 10^{-3} Pa), both at 1000°C/6h. Chalcogenide glass melting was carried out at 800°C/12 h with rocking to homogenize the melt. The melt was cooled to 650°C, held isothermally, statically and vertically for 2 h for melt-refining [16], quenched under a dynamic nitrogen (O_2-free, BOC) flow and then annealed *in situ* inside the melting ampoule, by heating isothermally at the chalcogenide glass T_g (extrapolated-onset from thermal analysis [17]) for 1.5 h, followed by slow cooling through the T_g region, then cooling to ambient *in situ* with the furnace turned off. The TeAsSe glass rod-preform, on removal from the silica ampoule, was fiber-drawn to mono-structured fiber of 145±5 μm OD (*outside-diameter*), on an in-house modified fiber-drawing tower (Heathway), housed in a Class 100,000 cleanroom.

B. Fabrication of TeAsSe fiber tapered-tips

(i) Propylamine wet-etchant

For propylamine wet-etching, 0.5 m of the TeAsSe fiber was freshly cleaved (Lunzer diamond-scribe) and hung vertically, with the fiber upper-end supported in a 20 mm long groove (200 μm x 200 μm) in an Al block. The Al block was supported in a 3-D (dimensional) optical stage to ensure the fiber hung centrally within the boiling tube holding the propylamine (82100-1, Fluka Analytical), and gave an accurate fiber immersion depth in the propylamine of 3 mm. The TeAsSe fiber was etched (24 h, 22 ±2°C). Straight after etching, the tip was gently sluiced in acetone (certified grade, Fisher) at room temperature and dried under dust-cover. 25 tips were individually prepared for comparison: each tip was mounted on a silicate glass microscope slide (*with Plasticine*©) for optical microscopy and on an Al stub using carbon tape for FEG scanning electron microscopy (FEG-SEM XL30, Philips).

(ii) Piranha solution wet-etchant

The TeAsSe fiber was etched under ambient air, at 22 ±0.1°C in Piranha solution following the method in section II 2. B. On average, 35±3min etching was required to reduce the 145μm OD TeAsSe fiber to a 4 μm aperture diameter; the etching rate was ~2 μm min^{-1}.

2. *AsSe-SIF Tapered-tips*

A. *Fabrication of AsSe-SIF*

The AsSe-SIF was prepared as in [18, 19] and comprised an $As_{34.9}Se_{65.1}$ at% core glass and $As_{29.3}Se_{70.7}$ at% cladding glass, with core OD/fiber OD of 28 μm / 235 μm. The AsSe-SIF was coated with fluoropolymer (F42), on-line, during fiber-drawing. The refractive indices of the core/cladding glasses were 2.73/2.68, respectively, at 3 μm wavelength, so NA=0.52; the measured NA was 0.2 at 1.56 μm [20].

B. *Fabrication of AsSe-SIF tapered-tips, using Piranha solution wet-etchant*

The As-Se SIF was etched in Piranha solution at 22 ±0.1°C, *e.g.* 50 ±2 min etching tapered the 235μm OD AsSe-SIF to a 4 μm aperture, so the etching rate was ~2.3 μm min^{-1}.

It should be noted that: (i) immediately prior to making up the Piranha wet-etchant, all glassware to be used was rinsed in high purity (reverse-osmosis) water and dried at 70°C for ≥ 15 min; (ii) the Piranha solution lost activity with time and so a fresh batch of 40 ml Piranha solution was prepared, then discarded, for etching each new fiber sample; (iii) all process steps were timed and timings adhered to, in order to make the tapered tips reproducibly and (iv) nitrile protective gloves were worn for all handling. The Piranha solution batch consisted of 3 parts by volume (12ml) hydrogen peroxide (H_2O_2, 30% w/v (100 volumes) aqueous solution, code: 452024T, Aristar, BDH) to 7 parts (28ml) sulfuric acid (H_2SO_4, S/9222/P13, specific gravity at ambient temperature 1.83 (>95%), electronic MOS Grade, Fisher). The$H_2O_2$was poured into a measuring cylinder (capacity 50 ml, Pyrex©, FisherBrand©). This measuring cylinder was then clamped in a beaker (capacity 600 ml, Pyrex©, FisherBrand©) on a magnetic stirrer/heater, holding 500 ml high purity water at 22±0.1°C acting as a constant-temperature water bath. The H_2SO_4 was measured in a separate measuring cylinder (capacity 50ml, FisherBrand©) and then poured gently into the H_2O_2, whilst stirring, using a silicate-glass rod. The reaction was exothermic; the temperature of the water bath reduced. After 10mins equilibration, 10ml of this Piranha solution was poured into the "etching-cylinder" (10mm ID and 10 ml capacity, Pyrex©, FisherBrand©) which was clamped in the constant water bath and left to equilibrate for 15min. The Piranha solution cleaned the etching-cylinder, as evidenced by the bubbling on contact. This aliquot of Piranha solution was discarded (with excess cold water) and a fresh10mlaliquot was poured into the etchant-cylinder, clamped in the constant water bath. 2, 6, 10, 14-tetra-methyl-penta-decane (TMPD, ~ 157 mm^3 volume, Acros Organics) was gently delivered *via* a teat pipette (Pyrex™©) onto the top of the Piranha solution, creating an immiscible surface-layer of ~ 2 mm depth, which not only minimised fuming of the Piranha solution but also helped to ensure the reproducibility of the tapered-tip geometry [7]. A visible-light microscope-camera (Discovery Veho, VMS-001) was clamped alongside the etching-cylinder to monitor the etching process.

Just prior to preparing the Piranha solution etchant as above, 0.5 m AsSe-SIF was freshly cleaved at each end (Lunzer diamond-scribe). The F42 polymer coating was stripped for 3 mm at one end of the fiber, by gently stroking the fiber with lens tissue soaked in acetone (certified grade, Fisher). The fiber was then threaded into an ID/OD=0.3±0.1 mm/2.0 ±0.1 mm, 0.45 m long hollow-core cane, made of sodium borosilicate glass, so that the 3mm of uncoated chalcogenide fiber protruded from the bottom end of the hollow-core cane, exposed ready for being etched, and a further 3 mm of the coated fiber protruded. The fiber was a snug fit inside the hollow-core cane, nevertheless the polymer-coated fiber, protruding from the top end of the hollow-core cane, was secured using Plasticine©, to prevent the fiber from slipping down through the hollow-core cane. (Note: the hollow-core cane was drawn in-house from sodium borosilicate glass tube (Simax) on the customized Heathway draw tower, in the class 100,000 cleanroom.) The hollow-core cane not only protected the chalcogenide fiber from inadvertent fracture but also helped to prevent fumes from the etchant attacking the upper fiber. The hollow-core cane, holding the chalcogenide fiber, was clamped vertically in a 3-axis optical stage (using a ceramic magnet (20x5x5 mm^3) so that the exposed chalcogenide fiber protruding from the bottom end of the hollow-core cane could be accurately positioned in the etchant to a depth of 4 mm, *i.e.* the end of the fiber lay 2 mm below the meniscus of the Piranha solution, while 2 mm of the fiber passed through the TMPDS immiscible layer lying on top of the Piranha solution (Fig. 1(a)). By then the Piranha solution was 25 mins old and was used immediately.

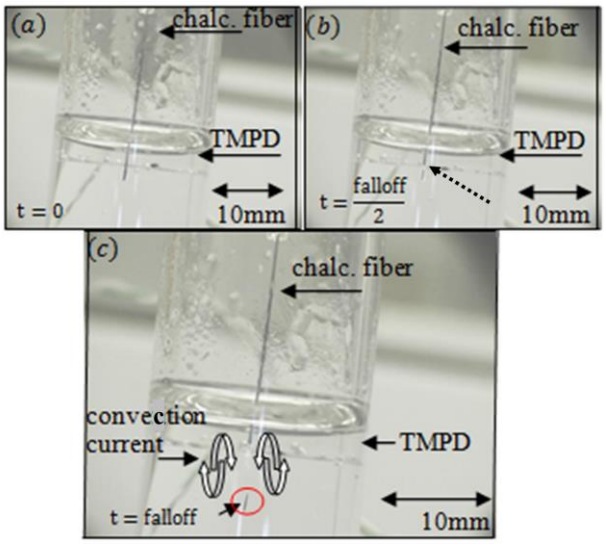

Figure 1. Microscope-camera images of Piranha wet-etching of AsSe-SIF. The immiscible TMPD layer, on top of the Piranha solution, shows clearly due to refraction. (a) At start-time, t_0, the fiber was immersed 2mm below the upper TMPD layer. (b) Mid-way through etching, $t_{fall\text{-}off/2}$, the fiber had necked down (see dashed arrow). (c) Moments after $t_{fall\text{-}off}$, the fiber had necked down sufficiently for the lower part to detach and slowly descend to the bottom of the etching-cylinder. Also in (c), the curved arrows on each side of the fiber illustrate the convection current setup in the Piranha solution.

During etching, colored Piranha solution immediately in contact with the fiber continuously sank and was replaced by fresh, colorless Piranha solution flowing in to replace it at the top near the interface of the TMPD and the Piranha solution. So, the Piranha solution layer was observed to be constantly

moving down parallel to the fiber surface (see Fig. 1(c)); Unger *et al.* [7] have described this as laminar flow. It is suggested that dissolution of the chalcogenide glass made the Piranha solution deeper in color and more dense, initiating this convection current (Fig. 1 (c)) which started in the uppermost area (near the TPMD layer) and moved down along the fiber length. Since the 'fresh' Piranha solution contacted the fiber first at the uppermost part, *i.e.* near to the TPMD interface with the Piranha solution, etching was fastest here[7] and necking down of the fiber occurred here. Eventually, the neck-down was sufficient such that the lowermost part of the fiber detached at the neck and sank slowly to the bottom of the etching-cylinder. This detachment is illustrated in Fig. 1(c) just after time: $t_{fall\text{-}off}$. Figs. 1(a) – (c) show images of the chalcogenide fiber AsSe-SIF captured with the microscope camera during the Piranha etching. Fig. 1(a) shows the straight-sided fiber at t_0(start-time).Fig. 1(b) shows the fiber mid-way through the etching, at $t_{fall\text{-}off/2}$, when necking down was proceeding. Finally, Fig. 1(c) captures the moment just after the neck had broken and the lower part of the fiber had detached and was falling away through the liquid to the bottom of the etching-cylinder beneath the clamped fiber, which was left now with a tapered-tip at the etched end.

At $\leq t_{fall\text{-}off}$ + 20 s, the fiber above the severed neck was removed from the Piranha solution and the etched end was washed gently in methanol (>99%, Fisher Scientific) and blown gently dry with N_2 ('white spot' O_2-free, BOC) passing through a small nozzle and directed off-axis relative to the fiber. The hollow-core cane was removed. Each 0.5 m AsSe-SIF, with a tapered-tip at one end, was individually stored under ambient conditions, under dust-cover.

The AsSe-SIF tapered-tips were imaged using optical microscopy by adhering a point further along the polymer coated fiber to a microscope slide, using Plasticine©. Tapered tips were also imaged using FEG SEM (Philip XL30) by mounting on a 30 mm OD Al stub using carbon tape.

III. Results of Etching

A. Propylamine etching

Figure 2 shows FEG-SEM imaging of a typical TeAsSe fiber after propylamine wet-etching. The tip-profile was asymmetric and the tip-surface roughened (surface of roughness *ca.*± 50 μm), with a deposit.

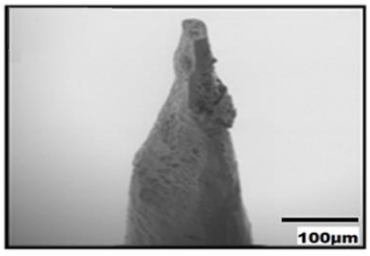

Figure 2. FEG-SEM micrograph of the side elevation of a typical TeAsSe fiber, after propylamine-etching showing asymmetrical tip-geometry and its roughened surface with a deposit.

B. Piranha etching

For Piranha etching, maintaining both an exact angle of 90°between the tapered-tip and the Piranha solution meniscus and exact immersion-depths were found mandatory, in order to achieve symmetrically tapered-tips. Fig. 3 (a) and (b) show optical, and FEG-SEM micrographs, of the typically smooth fiber tips obtained, here of aperture 4 μm.

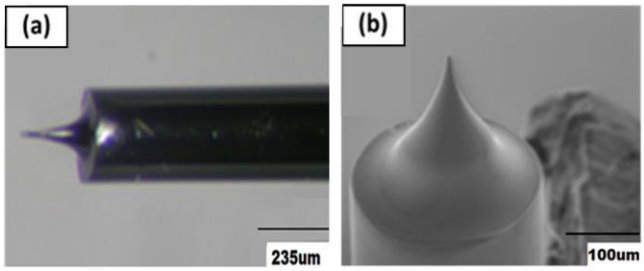

Figure 3. (a) Optical micrograph of a AsSe-SIF after 50 minutes Piranaha wet-etching, followed by immediate washing in methanol and blow-drying with N_2. (b) FEG-SEM micrograph of the same tapered-tip of tip-aperture diameter 4 μm.

Single, double and triple step-profiles were controlled dynamically, by adjusting the length of fiber immersed in the Piranha solution. Some step-profiles formed by retracting the fiber from the Piranha solution at specific times are shown in Fig. 4 (a)-(d). The length of a stepped-region was equal to the length of fiber retracted; the diameter of the stepped-region depended on the time that the fiber had been immersed in the Piranha solution for that step. Longer tapers required a longer section of the fiber to be immersed initially beneath the meniscus of the TMPD layer; shorter tapers required a shorter length to be immersed. The fabrication of: (i) single-step tapered; (ii) triple-step tapered; (iii) short tapered (e.g. ~100 μm) and (iv) longer tapered (up to 1110 μm) tips was reproducibly demonstrated with aperture diameters from 0.292 to ~4μm.

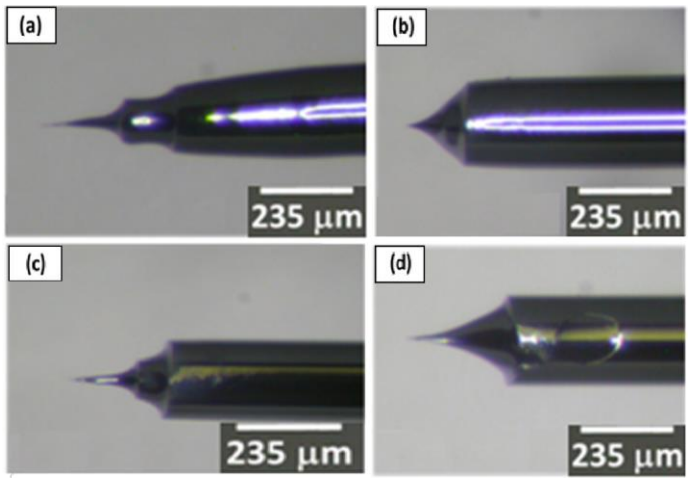

Figure 4. (a) – (d) Optical micrographs of Piranha wet-etched AsSe-SIF tapered-tips of different profiles; each could be prepared reproducibly. Note: tapered-tip (a) had no 'shoulders' and therefore during the line-of-site evaporative Al-coating, it was not possible to achieve a 'shadow' effect to prevent the tip-aperture from being coated (see section IV (A)).

IV. Optical behavior of Al-coated, Piranha Solution Etched, AsSe FIB Tapered-tips

A. Method of Al-coating

To ensure that the Piranha-etched, AsSe-SIF tapered SNIM tips (section III) accepted MIR light through the tip, yet prevented unwanted light from entering the sides of the tapered-tip, a metal coating was applied to the taper sides, but not to the tip end-aperture. Al has high optical density, yet ~ 96% reflectivity [21] across the MIR wavelength range 0.1-10μm, making it an effective metal coating for achieving both tasks. Furthermore, the metal coating offered the tip physical protection. Al (*vapor pressure ~10^{-5} Pa at normal melting point of 660℃* [22]) was placed in a silica-glass boat in an in-house evaporator. A 0.5 m long chalcogenide glass optical fiber, with a Piranha-etched tapered-tip, was threaded by hand through a sodium borosilicate glass hollow-core cane of 30 mm length and ID/OD = 0.3±0.01 mm/2.0 ±0.01 mm(made in-house, as in section II(2)B), so that the etched tapered-tip protruded 3 mm from one end of the hollow-cane. The hollow-cane with the 3 mm tip protruding was elevated to an angle of 30° with respect to the horizontal plane of the Al-target and was secured65mm distant from the Al target. The remaining fiber length was coiled into a loop of diameter ~ 16 mm to fit inside the thermal evaporator. The aim was to achieve not only a uniform Al-coating on the taper sides, and the taper 'shoulder' (*which was the taper profile as the taper rejoined the main fiber profile*), but also to shadow the tip-aperture, by line-of-sight at the tip-shoulder, to prevent the tip-aperture from being Al-coated. The fiber tapered tips were coated under 10^{-2} Pa in three consecutive stages, each lasting 2 s, with rotation of the fiber by 120° after each stage, in order to deliver a uniformly thick coating of Al of ~ 100 nm (Fig. 5).

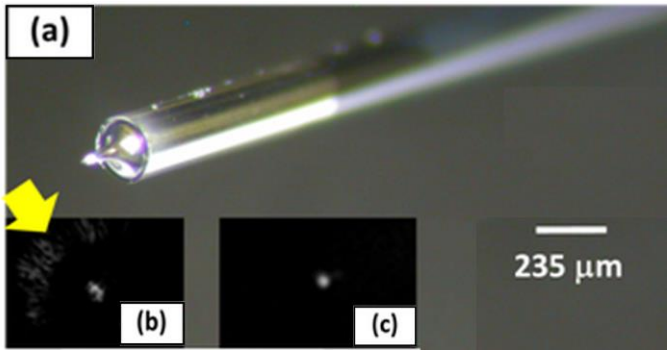

Figure 5. (a) Optical micrographs of a Piranha wet-etched AsSe-SIF tapered-tip of aperture: 4 μm OD, that had been Al-coated on the sides of the tip but not at the tip-aperture. It is suggested that the AsSeS optical cladding had been etched away by the Piranha solution to leave only the core AsSe glass at the tip-aperture. Inset (b): near-field image of 1550nm wavelength light exiting the tip, showing light leaking in a ring-like pattern, presumed escaping at the tapered tip 'shoulders'(see broad arrow), prior to the tip being Al-coated. Inset (c): light emerging only from the tip-aperture after the taper sides had been Al-coated.

A coating thickness calibration was carried out by placing a silicate-glass microscope slide vertically, adjacent to the fiber tip, at the same height and distance from the Al-target, so that the slide was coated at the same time as the tip and received a similar depth of condensing Al-vapor, measured to be 99 ±6 nm using FEG-SEM after the evaporation process.

B. Optical behavior

Optical transmission of the AsSe-SIF tapered tips before, and after, the Al-coating was investigated. A 4 mW at 1550nm, continuous-wave laser (81980A, Agilent) was coupled, *via* a commercial tapered silica glass optical fiber, into the plain end (*i.e. end of fiber remote from the tip*) of the AsSe-SIF, whose other end had been Piranha-etched to form a tip-aperture. The laser-light was collected from the tip-aperture of the tapered end of the AsSe-SIF (Fig. 5(b) and (c))using a x10 microscope objective (0.25NA, Newport), which was focused onto a near-infrared (NIR)camera (XQ1112, Siemens) and displayed on a cathode-ray-tube monitor. In addition, the reverse optical circuit was tested; thus light was launched into the fiber tip-aperture and its exit at the plain end of the fiber was monitored in the near-field. It was assumed that the AsSeS glass optical cladding had been etched away to leave the AsSe core only in the tip, since the tip aperture here was only 4 μm, and the fiber core diameter had been 28 μm. This assumption depended on the tip-aperture and the fiber core being concentric. Inset (b) of Fig. 5 shows a near-field image of the NIR light (1550nm, 4mW) emerging from the same tip before it had been Al-coated. The objective lens (x10, 0.25NA, Newport) was focused onto the ring of radiation leaking *via* the shoulders of the same tip. Inset (c) of Fig. 5 shows the NIR light successfully emitted only by the tip-aperture, after the taper sides had been Al-coated. That the light was confined and exiting the tip-aperture suggests that the Al coating thickness applied was adequate in terms of not only preventing light prematurely emerging from the shoulders of the tip, but also confining light propagating in the tapered-tip. The reverse optical circuit also successfully guided light launched into the tip-aperture to exit at the opposite, plain end of the fiber.

V. FIB cleaving of the tip-aperture, AsSe-SIF tapered-tips

A. Method of FIB etching

A 0.5 m long AsSe-SIF was Piranha-etched (section II(2)B) to create a tapered-tip of aperture 292 nm. *Ca.*100 nm of Al was deposited on the sides of the tapered tip (following the method in section IV A). Taking the end of the fiber which had been Piranha-etched and Al-coated, 30 mm of the fiber measured from the tapered-tip, was mounted flat using a carbon tape onto an Al stub (30mm diameter, circular, disposable) and the stub was placed on the 5-axis motorized stage in the chamber of the Focused Ion Beam (FIB) miller (FEI Quanta 200 3D). The rest of the fiber length (470mm) was coiled in a loop (radius ~7mm) and secured with copper tape under the 5-axis motorized stage inside the FIB chamber. The antechamber of the FIB was then evacuated to 10^{-4}Pa and then the tapered-tip was oriented (using the 5-axis motorized stage) to be perpendicular to the high beam current gun inside the FIB

antechamber. Due to the unique composition of the AsSe-SIF, no suitable pre-calibrated setting for FIB milling existed on the control system. Instead a GaAs milling setting (1 µs dwell time, 19.5nm pitch, 30 kV, 0.30 nA) was selected as being a reasonable guide, to calibrate the FIB; this automatically set the volume-per-dose value (*i.e.* sputter/mill rate: μm^3/nC) of the Ga ion column. The Al-coated, Piranha-etched tapered-tip was selectively aligned with the high beam current gun at the point at which the tip-diameter was 20µm, aiming to fabricate a 20µm diameter tip-aperture (Fig. 6(a)).

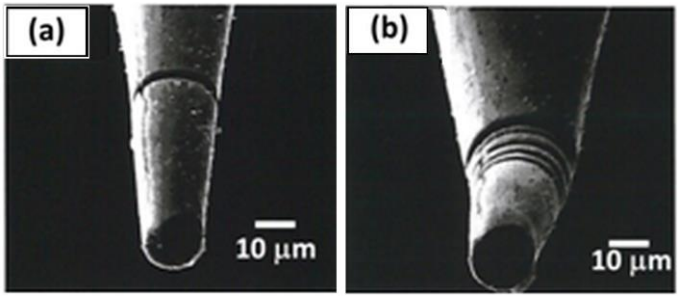

Figure 6. FEG-SEM images of Al pre-coated, AsSe-SIF, tapered-tip after first attempts to calibrate the FIB current and milling rate: (a) actual area milled, but fiber tip remained attached; (b) five attempts to cleave the fiber failed with the fiber bent upwards and would not drop away.

Initially, it was found that the presence of the Al-coating adversely affected the ability to FIB cleave the tip compared to having no Al-coating. The FIB milled tip would not come cleanly away from the milled aperture (Figs. 6(b). It was concluded that pre-coating the tip with Al prior to FIB milling inhibiting it from falling away, presumably because the Al-coating had strengthened the fiber. With further exploration, the FIB conditions were determined for successful cleaving of a flat aperture on Al-coated tapered tips (see Fig. 7). The fiber tip detached below the milled point, to leave the 20 µm aperture diameter, as desired (Fig.7).Then, four consecutive lower probe "polishing" currents of 0.5nA, 0.3nA, 0.1nA and 0.01nA (30k accelerating voltage, GaAs setting) of the FIB to polish the newly cleaved, AsSe-SIF tapered tip, while the tip was still mounted onto the stub and inside the FIB chamber, in order to remove any residual roughness features introduced during the milling. To achieve resolutions of the order of 100 nm requires that the FIB-produced chalcogenide glass tips are made smaller than the 20 µm diameter aperture manufactured here. The FIB manufacturing technique has the potential advantages of controllability, and so tip reproducibility, and tip-aperture high quality. There is no reason *per se* why the FIB chalcogenide glass tips should not be made, 'to order', much smaller in sub-aperture.

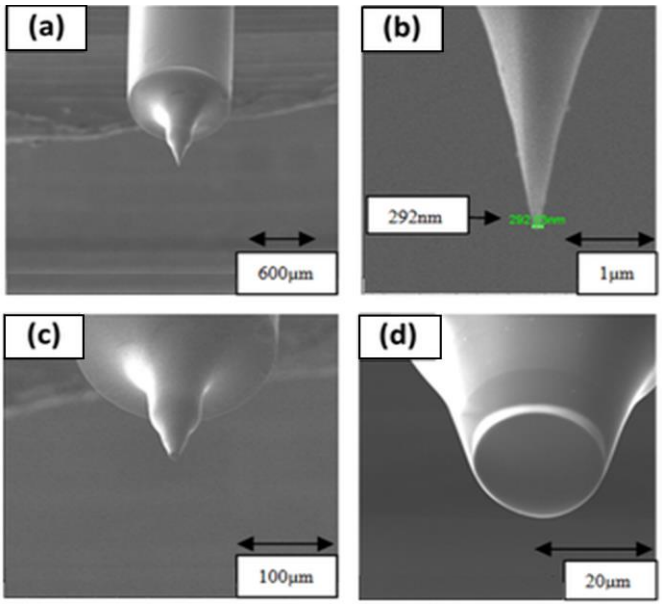

Figure 7. FEG-SEM images of a Piranha wet-etched tip. The tip had been mounted on a stub inside the FIB chamber: (a) side elevation view of the tapered-tip after wet-etching in Piranha to a tip-aperture 292nm OD and Al-coating, and before it was FIB milled to cleave to produce a 20µm diameter aperture; (b) close-up of tip-aperture shown in (a)indicating tip-aperture OD; (c) the newly formed tip-aperture, of the tapered-tip shown in (a) and (b), after it had been cleaved using the FIB milling to the pre-selected 20µm diameter. (d) after the tip-aperture was subsequently "polished" four times with beam currents of 0.5nA, 0.3nA, 0.1nA and 0.01nA, respectively (all at 30kV beam acceleration voltage and GaAs setting).

After the milling had been completed, images were taken by means of FEG-SEM (see Figs.7(c) and (d)) with the tip still inside the FIB antechamber. Fig. 7(c) shows the AsSe-SIF tip after having being FIB milled (*i.e.* cleaved). Fig.7 (d) shows a close up image of the same tip and shows that the FIB has produced a flat ~20µm OD aperture; Fig. 7(b) indicates that the original tip-aperture, before the FIB milling, had a sub-micron diameter of 292 nm. The surface of the tip-aperture, formed by the FIB milling, did not appear rough at the highest magnification on the FIB. FEG-SEM EDX analysis indicated that Al was absent from the FIB cleaved aperture of the AsSe-SIF tapered-tip, so yielding a clean optical aperture for receiving MIR light during SNIM. Because the 20 µm aperture was created 'on-demand' by FIB milling, then it is surmised that any aperture ($A_{selected}$) may be chosen and readily fabricated 'to order' using FIB, whereby: $A_{etched\text{-}aperture} < A_{selected} \leq A_{fiber\text{-}core.}$ In other words, the outside limits of the selected aperture would be not smaller than the initially Piranha-etched aperture and not bigger than the fiber-core diameter. The latter limit matters if light confined to the fiber optical core is required along the remaining fiber as the MIR light travels along the fiber having entered at the fiber tapered-tip tip-aperture.

VI. Acquisition of MIR spectra of cells using a FIB-cleaved tip

The FIB-cleaved tip (Fig. 7(d)) at one end of the MIR optical fiber As-Se SIF was used to collect preliminary MIR transflection spectra of individual cells at the Beamline 22

(B22-Infrared) of the Diamond Light synchrotron, Oxfordshire, UK. Cells (colon cancer cell-line, DLD) had been mounted and fixed on a MIR reflective glass slide (Kevley) for MIR transflection spectroscopy. The cell slide sample was 12 months old and was kindly provided by B22 Beamline Scientist Dr K Wehbe (the cell sample was designated by Dr Wehbe as *DLD 14 on MIRR IR (double) ff4%, dated 22/11/11*).

Figure 8(a) shows a schematic of the optical circuit used at the B22 source, which was based on free-space optics. The incoming B22 beam was passed through the interferometer of a FTIR (Fourier transform infrared) spectrometer (Vertex 80 V, Bruker) and then focused onto the cell-sample, *via* an off-axis parabolic mirror.

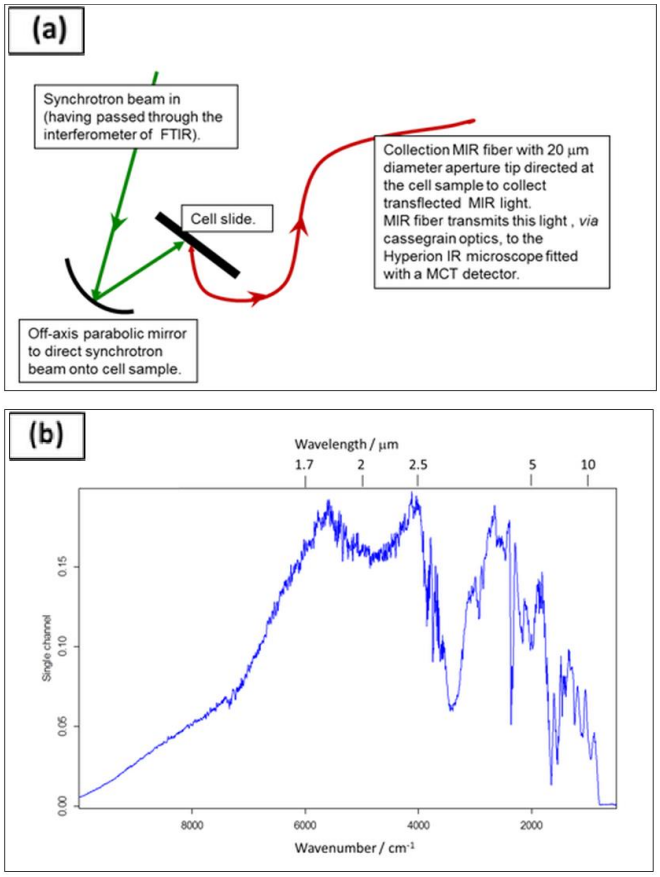

Figure. 8 (a) Schematic arrangement of the optical set-up to collect cell spectra *via* the MIR fiber and FIB cleaved and polished fiber tip of 20 μm aperture (see Fig. 7(d)). (b) typical transflection spectrum (*averaged over 5 mins/ 8 cm^{-1} resolution, with FTIR center-burst amplitude of 13700 A, not ratioed to a background*) of a 40 μm diameter, round cell. Spectral absorption bands present include amide I (5.92-6.15 μm wavelength *i.e.* 1689-1626 cm^{-1}) and amide II (6.45 μm wavelength *i.e.* 1550 cm^{-1}) bands as would be expected.

In addition, two microscope-cameras were placed orthogonally and located so that they were close enough to be capable of visually imaging the cells mounted on the slide substrate. The cell-slide was supported on a 3-axis optical stage so that the cells could be positioned carefully relative to the B22 beam. The 20 μm diameter MIR fiber tip aperture (Fig. 7(d) and section V), used to collect the MIR light after transflection through a cell, could be brought very close to a selected cell without touching the cell.

MIR transflection spectra were collected for various collection times from 5 minutes to 7 hours and a wavenumber resolution of either 4 or 8 cm^{-1}. The FTIR amplitude of center-burst ranged from 6000A to 13700A. Spectra from seven different cells were collected, and many spectra were repeated. Fig. 8(b) shows a typical result of an averaged spectrum of a cell, collected using the 20 μm aperture, FIB-cleaved MIR tip, here for 5 mins/8 cm^{-1} resolution, with center-burst amplitude 13700 A. This particular cell according to the microscope-cameras was of round morphology and diameter 40 μm. The spectrum shown in Fig. 8(b) was not ratioed to a background and comprised a promising detailed set of spectral absorption including of amide I (5.92-6.15 μm wavelength *i.e.* 1689-1626 cm^{-1}) and amide II (6.45 μm wavelength *i.e.* 1550 cm^{-1}). Atmospheric water (2.9 μm) and CO_2 (4.2 μm) bands were observed due to the free-space optical set-up.

VII. Conclusions

An investigation into wet chemical etching of unstructured and structured chalcogenide glass fibers was undertaken with the aim of producing a tip suitable for MIR scanning near-field microscopy (SNIM) of human cells and tissue and other molecular samples. It was found that wet-etching in propylamine produced asymmetric tips and uncontrolled tip geometries. The tips formed had a long (2 mm) and uneven (± 50 μm) tapering region, and exhibited deformations and rough surfaces. Long etching times were required, of ≥ 24h at room temperature.

On the other hand, excellent quality chalcogenide optical fiber tapered-tips of reproducible geometry were fabricated using Piranha solution wet-etching in a dedicated rig and with the developed methodology. The rig maintained an exact angle of 90°between the tapered-tip and the Piranha solution meniscus, and an exact immersion-depth, in order to achieve symmetrically tapered-tips. Chalcogenide-glass, optical-fiber tapered tips of single-, double- and triple- stepped geometries were reproducibly made, with the length of the tapered-tip ranging from 100 – 1110μm, and aperture diameters ranging from ~ 0.3-4μm. Al coatings of 100 nm depth were applied to the tapered sides and shoulders of the tapered-tips but not to the tip-aperture. The Al coatings were found to be of sufficient depth and coverage to confine light within the tapered-tip. A novel approach was invented here. Thus FIB milling was used to cleave the Piranha-etched tips to produce an aperture which was flat, smooth, orthogonal to the fiber axis, and of exactly the chosen aperture. Low probe currents were employed to FIB 'polish' the aperture to the nm-scale. The FIB cleaved tip was used to gather transflection spectra from fixed cells under illumination of a synchrotron-generated MIR broadband beam. Other MIR applications where fiber tapering is required may also benefit from the FIB-cleave-polish procedure described here.

ACKNOWLEDGMENT

G.S.A. acknowledges, with thanks, the financial support received from EPSRC (Engineering and Physical Research Council), UK, and The University of Nottingham, UK. The Authors acknowledge the input of Dr Giancarlo Felice, Beamline 22 Principal Scientist at the Diamond Light Synchrotron who introduced the ideas of SNIM to the Authors and has been an inspiration in their work.

REFERENCES

[1] E. Abbe, "The relation of aperture and power in the microscope," *J. Royal Microscopical Soc.*, vol. 2, no. 3, pp. 300-309, 1882.

[2] V. L. Mironov, *Fundamentals of Scanning Probe Microscopy*. NT-MDT, Nishny Novgorod, Russian Federation, 2004.

[3] J.S.Sanghera, I.D. Aggarwal, A. Cricenti, R. Generosi, M. Luce, P. Perfetti, G. Margaritondo, N.H. Tolk and D. Piston, "Infrared scanning near-field optical microscopy below the diffraction limit", *IEEE J. Sel. Top. Quant. Electron.*, vol. 14, no. 5, pp. 1342-1352, 2008.

[4] A.Cricenti, R. Generosi, M. Luce, P. Perfetti, G. Margaritondo, D. Talley, J. S. Sanghera, I. D. Aggarwal, J. M. Gilligan, and N. H. Tolk, "Spectroscopic scanning near-field optical microscopy with a free electron laser: CH_2 bond imaging in diamond films," *J. Microscopy*, vol. 202, no. 2, pp. 446-450, 2001.

[5] D. B. Talley, L. B. Shaw, J. S. Sanghera, I. D. Aggarwal, A. Cricenti, R. Generosi, M. Luce, G. Margaritondo, J. M. Gilligan, and N. H. Tolk, "Scanning near-field infrared microscopy using chalcogenide infrared tips," *Mat. Lett.*, vol. 42, pp. 339-344, 2000.

[6] D.T. Schaafsma, R. Mossadegh, J. S. Sanghera, I. D. Aggarwal, M. Luce, R. Generosi, P. Perfetti, A. Cricenti, J. M. Gilligan and N. H. Tolk, "Fabrication of single-mode chalcogenide fiber probes for scanning near-field infrared optical microscopy," *Opt. Eng.*, vol. 38, no. 8, pp. 1381-1385, 1999.

[7] M. A.Unger, D. A. Kossakovski, R. Kongovi, J. L. Beauchamp, and J. D. Baldeschwieler, "Etched chalcogenide fibers for near-field infrared scanning microscopy," *Rev. Sci. Instrum.*, vol. 69, no. 8, pp. 2988-2993, 1998.

[8] C. R. Petersen, U. Møller, I. Kubat, B. Zhou, S. Dupont, J. Ramsay, T. M. Benson, S. Sujecki, N. Abdel-Moneim, Z. Tang, D. Furniss, A. B. Seddon and O. Bang, "Mid-infrared supercontinuum covering the 1.4 - 13.3 μm molecular fingerprint region using ulta-high NA chalcogenide step-index fibre," *Nat. Photonics*, vol. 8, pp. 830-834, 2014.

[9] Y. Yu, B. Zhang, X. Gai, C. Zhai, S. Qi, W. Guo, Z. Yang, R. Wang, D.-Y. Choi, S. Madden and B. Luther-Davies, "1.8 to 10 μm mid-infrared supercontinuum generated in a step index chalcogenide fiber using low peak pump power," *Opt. Lett.*, vol. 40, no. 6, pp. 1081-1084, 2015.

[10] H. A. Bectel, E. A. Muller, R. L. Olmon, M. C. Martin, and M. B. Raschke, "Ultrabroadband infrared nanospectroscopic imaging," *Proceedings of the National Academy of Sciences of the United States of America (PNAS)*,vol. 111, no. 20, pp. 7191-7196, 2014.

[11] M. Diem, S. Boydston-White and L. Chiriboga, "Infrared spectroscopy of cells and tissues: shining light onto a novel subject," *Appl. Spectroscopy*, vol. 53, no. 4, pp. 148A-161A, 1999.

[12] A. B. Seddon, "A prospective for new mid-infrared medical endoscopy using chalcogenide glasses," *Int. J. Applied Glass Sci.*, vol. 2, no. 3, pp. 177–191, 2011.

[13] D. Lezal, J. Zavadil, L. Horak, M. Prochazka and M. Poulain, "Chalcogenide glasses and fibers for applications in medicine," *Proc. SPIE 4158, Biomonitoring and Endoscopy Technologies*, vol. 124, 2001, doi:10.1117/12.413785.

[14] A. R. Hilton, *Chalcogenide Glasses for Infrared Optics*. McGraw-Hill Professional Publishing, USA, 2009.

[15] Z. Tang, V. S. Shiryaev, D. Furniss, L. Sojka, S. Sujecki, T. M. Benson, A. B. Seddon and M. F. Churbanov, "Low loss Ge-As-Se chalcogenide glass fiber, fabricated using extruded preform, for mid-infrared photonics," *Opt. Mat. Exp.*, vol. 5, issue 8, pp. 1722-1737, (2015).

[16] D. I. Aggarwal, R. Mossadegh, C. P. Pureza and J. Sanghera, "Process for making optical fibers from core and cladding glass rods," U.S. Patent ADD019376, Mar. 9, 1999.

[17] D. Furniss and A. B. Seddon, "Thermal Analysis of Inorganic Compound Glasses and Glass-Ceramics," in *Principles and Applications of Thermal Analysis*, P. Gabbott, Ed. Blackwell Publishing Ltd., UK, 2008., pp. 411-442.

[18] M.F. Churbanov, V. S. Shiryaev, I. V. Skripachev, G. E. Snopatin, V. G. Pimenov, S. V. Smetanin, R. M. Shaposhnikov, I. E. Fadin, Yu N. Pyrkov and V. G. Plotnichenko, "High-purity $As_2S_{1.5}Se_{1.5}$ glass optical fibers," *Inorganic Materials*, vol 38, no. 2, pp. 193-197, 2002.

[19] M. Churbanov, V. Shiryaev, A. Suchkov, A. Pushkin, V. Gerasimenko, R. Shaposhnikov, E. Dianov, V. Plotnichenko, V. Koltashev, Y. Pyrkov, J. Lucas and J. Adam, "High-purity As-S-Se and As-Se-Te glasses and optical fibers, " *Inorganic Materials*, vol. 43, no. 4, pp. 441-447, 2007.

[20] L. N. Blinov, L. N. Izmailova, L. A. Baidakov, L. P. Strakhov, "Determination of refractive index for a number of compositions of As-Se system," *Vestnik Leningradskogo Universitet*, vol. 16, pp. 142-145, 1967 [in Russian].

[21] J. Bartl and M. Baranek, "Emissivity of aluminium and its importance for radiometric measurement," *Measurement Sci. Rev.*, vol. 4, sec. 3, pp. 31-36, 2004.

[22] C. L. Yaws, *Handbook of Vapor Pressure, Inorganic Compounds and Elements.* Vol. 4, Gulf Professional Publishing, 1985.